Silver Nanoparticle-Embedded Polymersome Nanocarriers for the Treatment of Antibiotic-Resistant Infections

Journal:	*Nanoscale*
Manuscript ID:	NR-ART-10-2014-005823.R1
Article Type:	Paper
Date Submitted by the Author:	19-Dec-2014
Complete List of Authors:	Geilich, Benjamin; Northeastern University, Bioengineering van de Ven, Anne; Northeastern University, Physics Singleton, Gloria; Northeastern University, Chemical Engineering Arango, Liuda; Universidad de Antioquia, Sede de Investigación Universitaria (SIU), Grupo Biotecnología Sridhar, Srinivas; Northeastern University, Physics Webster, Thomas; Northeastern University, Chemical Engineering

SCHOLARONE™
Manuscripts

Silver Nanoparticle-Embedded Polymersome Nanocarriers for the Treatment of Antibiotic-Resistant Infections

Benjamin M. Geilich[1], Anne L. van de Ven[2], Gloria L. Singleton[3], Liuda J.S. Arango[4], Srinivas Sridhar[2], and Thomas J. Webster[3,5]

Departments of [1]Bioengineering, [2]Physics, and [3]Chemical Engineering, Northeastern University, Boston, MA 02115 USA; [4]Universidad de Antioquia, Grupo Biotecnología, Sede de Investigación Universitaria (SIU), AA 1226 Medellín, Colombia; [5]Center of Excellence for Advanced Materials Research, King Abdulaziz University, Jeddah, Saudi Arabia

ABSTRACT

The rapidly diminishing number of effective antibiotics that can be used to treat infectious diseases and associated complications in a physician's arsenal is having a drastic impact on human health today. This study explored the development and optimization of a polymersome nanocarrier formed from a biodegradable diblock copolymer to overcome bacterial antibiotic resistance. Here, the polymersomes were designed with silver nanoparticles embedded in the particle's hydrophobic membrane bilayer, and an antibiotic solution encapsulated in the particle's aqueous core in order to provide a dual-mechanism, concentrated, and less cytotoxic

localized treatment. These silver nanoparticle-embedded polymersomes (AgPs) were loaded with ampicillin and subsequently tested for bactericidal function against *Escherichia coli* that had been transformed with a gene for ampicillin resistance (*bla*). Results showed for the first time that AgPs killed the antibiotic-resistant bacteria, whereas free antibiotic, encapsulated antibiotic without the addition of the silver nanoparticles, and AgPs without the addition of ampicillin did not kill the bacteria. In this manner, this study introduces a novel nanomaterial that can effectively treat problematic, antibiotic-resistant infections in an improved capacity which should be further examined for a wide range of medical applications.

Keywords: polymersome; silver nanoparticle; antibiotic-resistance; *Escherichia coli*; ampicillin; nanomedicine

INTRODUCTION

Antibiotics have been extensively used since their commercialization in the 1930s to treat patients suffering from a wide variety of infectious diseases. When utilized correctly, these drugs are extremely effective at reducing mortality rates and healing time, which makes them essential in the clinic today. Unfortunately, however, antibiotics have been used so prevalently over the last 80 years that the bacteria they were designed to kill have begun to evolve and adapt, rendering these drugs ineffective.[1,2] According to the Center for Disease Control's 2013 report on antibiotic resistance in the United States, at least 2 million people acquire serious infections from antibiotic resistant bacteria each year, and over 23,000 die as a direct result.[3] Even when alternative treatments exist, patients with antibiotic resistant infections have significantly higher

mortality rates, and survivors often have increased hospital stays and long-term complications. These infections cost an estimated $20 billion in excess direct healthcare expenses.[3] Infections caused by Gram-negative bacteria are particularly difficult to treat because their robust and hydrophobic outer lipopolysaccharide membrane helps to impede the influx of drugs into the cell.[4] Of additional concern is the appearance of bacterial strains that are resistant to multiple types of antibiotics (known as multi-drug resistant or MDR strains). Clinicians are now discovering examples of bacteria with such diverse antibiotic-resistance that no available drug can successfully treat the infections they cause.[4] In essence, the near future will bring a new generation of "super bugs" that scientists and doctors do not know how to kill effectively. Unfortunately, the number of new antibiotic drugs in the pipeline has also been rapidly decreasing, largely due to the fact that new drugs are extremely expensive to bring to market, and antibiotics are less financially lucrative to develop when compared to treatments for chronic conditions.[5] Thus, the need to develop alternative strategies to treat such antibiotic-resistant bacteria, while still utilizing existing drugs, has never been more urgent than today.

Over the past decade, interest in using nanomedicine-based approaches to combat difficult infections has rapidly grown due to the many advantages offered over conventional treatment with free antibiotics. This study explored encapsulating the drug inside nano-sized structures called polymersomes (that is, artificial vesicles made from biodegradable, high molecular weight, amphiphilic block co-polymers). These vesicles typically display a spherical morphology and are composed of hydrated hydrophilic coronas both at the inside and outside of a hydrophobic polymer membrane.[6] This allows for hydrophilic bioactive materials to be loaded into the particle's aqueous core, and hydrophobic bioactive materials to be loaded into the particle's membrane bilayer. Just loading these compounds into carriers can provide many

benefits over treatment with free drugs. For example, encapsulation of antibiotics has been shown to protect the drug from critical bacterial resistance mechanisms such as degradation by ß-lactamase enzymes.[7] In one such study, Nacucchio *et al.* found that the liposomal encapsulation of piperacillin prevented staphylococcal ß-lactamases from hydrolyzing the drug.[8] Additionally, encapsulation has been demonstrated to facilitate a longer and sustained contact time between the antibiotic and the bacterial cell membrane.[9]

Along these lines, metallic nanoparticles have long been investigated as potential antibacterial agents due to their many unique physiochemical properties which are not present at the macro scale.[10] Among these metals, silver is perhaps the most well-known for its antimicrobial effects. Hippocrates noted its ability to enhance wound healing and preserve food and water as early as 400 BC, and many products taking advantage of these properties are available commercially today.[11-12] In addition, recent studies have shown that there may even be a synergistic effect when silver nanoparticles and antibiotics are used simultaneously to treat a Gram-negative infection.[13-15] However, there is little information regarding whether a combined treatment is sufficient to overcome bacteria which display genetic antibiotic resistance. Additionally, there has been almost no investigation into the effect of dually encapsulated antibiotics and nanoparticles. Researchers have also theorized that nanoparticles with a hydrophobic functionalization can include into lipid membranes and cause disruption, whereas their hydrophilic counterparts can only adsorb to the surface.[16] Again, the difficulty of successfully delivering hydrophobic nanoparticles without significant aggregation in an aqueous environment has limited investigation into the implications such a functionalization would have on the nanoparticles' antibacterial efficacy and cytotoxicity.

Thus, for all of the above reasons, the objective of the present *in vitro* study was to design, characterize, and optimize a polymersome nanocarrier able to co-localize and deliver both antibiotics and hydrophobic silver nanoparticles, while protecting the drug from hydrolysis by β-lactamase enzymes, in one "nanoformulation" in order to kill antibiotic-resistant bacteria. Specifically, these particles were then tested for efficacy against a strain of *Escherichia coli* (*E. coli*) which had been genetically modified to be antibiotic-resistant.

RESULTS

<u>Particle Design, Synthesis, and Characterization</u>

A diblock copolymer of methoxypoly(ethelyne glycol)$_{5,000}$ and poly(*D)-(L)*-lactic acid$_{50,000}$ (mPEG-PDLLA 5,000:50,000 Da) was utilized for the polymersome synthesis. The mPEG block was chosen because it has been documented to confer a "stealth" property to the particles *in vivo* in order to help prevent premature clearance by the immune system.[17] The racemic mixture of *D*- to *L*-lactides in the PDLLA block was optimized to generate polymersomes with a release rate sensitive to changes in temperature.[18] This allows for increased stability (low release) during storage at 4 ºC, and increased release at physiological temperatures.

Silver nanoparticle-embedded polymersomes (AgPs) were synthesized using a modified stirred-injection technique. Monodisperse hydrophobic silver nanoparticles of 5 nm diameter were suspended in an organic solvent containing dissolved mPEG-PDLLA. This mixture was injected through a syringe atomizer at high speed into actively stirring phosphate buffered saline (PBS, pH 7.4) containing the antibiotic ampicillin. The resulting suspension was allowed to dialyze against PBS to remove the organic solvent and non-encapsulated drug (Figure 1).

Physicochemical characterization was performed to assess AgPs size, surface charge, and loading. Transmission electron microscopy (TEM) revealed polymersomes of highly uniform size and shape with clusters of silver nanoparticles embedded inside (Figure 2A). These silver clusters frequently appeared as a single layer of nanoparticles that was off-center from the nanoparticle core, suggesting that they may be intercalated into the membrane bilayer. Dynamic light scattering (DLS) indicated the average hydrodynamic diameter to be 104.3 nm ± 15.6 nm (Figure 2B). The AgPs surface was found to have a near neutral zeta potential of 0.315mV ± 1.13mV at pH 7.4. The number of silver nanoparticles embedded per polymersome was quantified from TEM images. The nanoparticles were shown to load in a normal tailed distribution with an average of 9.29 ± 6.07 silver nanoparticles per polymersome (Figure 2C). The mass of silver loaded was estimated using the density of silver and the volume of a 5 nm sphere (Table 1, Equations 1-4).

Three different AgPs formulations were synthesized to contain different concentrations of ampicillin. The loading efficiency of ampicillin in the aqueous phase was measured by spectrophotometry as previously described.[19] The final ampicillin concentration following particle dialysis was determined to be 70µg/mL ± 7.0µg/mL, 110µg/mL ± 7.2µg/mL, and 160µg/mL ± 9.0µg/mL, corresponding to a loading efficiency of 23%, 22%, and 20%, respectively (Figure 2D). The final silver-to-ampicillin molecule ratio for the different AgPs formulations was 1:0.28, 1:0.44, and 1:0.64, respectively.

Bacterial Growth Inhibition

E. coli is a Gram-negative, rod-shaped bacterium which has been extensively investigated in the laboratory for over 60 years, making it one of the most widely studied prokaryotic

organisms and thus ideal for a proof-of-concept application. First, *E. coli* was transformed with a plasmid containing the *bla* gene encoding for the enzyme TEM-1 ß-lactamase using calcium chloride and heat-shock.[20] TEM-1 is the most common ß-lactamase found in enterobacteriaceae, and confers resistance to multiple antibiotics including the narrow-spectrum cephalosporins, cefamandole, cefoperazone, and all of the penicillins except for temocillin.[21]

The growth and proliferation of a 10^6 colony forming units/mL (CFU/mL) suspension of the ampicillin-resistant *E. coli* was examined by measuring the optical density at 600 nm (OD_{600}) for 24 hours following treatment with volumes of AgPs containing a silver:ampicillin (Ag:Amp) ratio of 1:0.28 (Figure 3A), 1:0.44 (Figure 3B), or 1:0.64 (Figure 3C). Ampicillin-loaded AgPs displayed significant bacteriostatic action against the *E. coli*, manifesting as a delay in the time taken to reach exponential growth phase. This response was dose-dependent, with higher concentrations of ampicillin producing a longer delay in bacterial growth. Bacteria treated with ampicillin concentrations above 55 µg/mL failed to proliferate within 48 hours. In the absence of silver nanoparticles, no bacteriostatic effect was observed for all ampicillin concentrations tested. This suggests that the presence of silver potentiates the therapeutic efficacy of ampicillin. AgPs without ampicillin likewise produced no therapeutic benefit. Additionally, no significant differences were observed between bacteria treated with free ampicillin (200 µg/mL), PBS, AgPs without ampicillin, and ampicillin-loaded polymersomes (200 µg/mL) without silver nanoparticles. When bacteria were treated with sub-optimal concentrations of AgPs, bacteria growth was always observed within 17 hours. The time to exponential phase was found to vary with both silver concentration and ampicillin loading (Figure 3D).

A Bliss Model was utilized to determine the degree of synergy observed for different

silver and ampicillin combinations.[22-23] Drug interactions were found be synergistic ($S>0$) in all cases where ampicillin was supplied at concentrations of 24 µg/mL and above (Figure 3E). At lower concentrations, no synergism was observed ($S=0$). The degree of synergy was dose-dependent and increased with both silver and ampicillin concentrations. The therapeutic benefit of ampicillin reached a plateau at 50 µg/mL over a range of silver concentrations due to complete inhibition of bacterial growth. When the silver concentration was held constant, the degree of synergism was directly determined by the amount of ampicillin loaded. This phenomenon is highlighted, in Figure 3F, where the bars indicate the range of synergism that can be achieved by varying ampicillin loading at a fixed silver concentration.

Cell-Particle Interactions

Interactions between *E. coli* and AgPs were visualized using TEM (Figure 4). Indentation of the bacterial cell membrane was observed in regions of AgPs contact (Figure 4B-C; white arrows). Silver nanoparticles inside AgPs appeared to be polarized in an orientation perpendicular to the bacterial cell membrane, suggestive of hydrophobic interactions with the outer cell membrane (Figure 4B, D; yellow arrows). In order to assess physical intracellular changes caused by AgPs, cells treated with an intermediate particle concentration (44 µg/mL Amp, 1 Ag:0.44 Amp) for 24 hours were sectioned. Bacteria in contact with AgPs displayed significant protein aggregation and diffuse widening of the cell envelope (Figure 4E-H). This phenomenon has been observed by other researchers following silver ion treatment, and has been shown to correlate with increased membrane permeability and protein misfolding due to disulfide bond disruption.[22,24-25] Regions of the cell envelope with little to no AgPs contact appeared morphologically normal (Figure 4F-H; black arrows).

The cytotoxicity of AgPs to mammalian cells was investigated using CCL-110 human dermal fibroblasts (Figure 5). Cells were treated with different concentrations of AgPs for 24 or 48 hours, and cell viability was measured using MTS assay. No significant cytotoxicity was observed over a range of 0-80 µg/mL ampicillin, 0-125 µg/mL silver.

DISCUSSION AND CONCLUSION

Prevention of cellular access of a drug is critical to antibiotic resistance, especially for Gram-negative bacteria because their robust outer lipopolysaccharide membrane provides an extremely effective permeability barrier.[26-28] In addition, *E. coli* possess efflux pumps (AcrB) which can help to remove antibiotics from the cell.[29] When bacteria possess genetic resistance, the antibiotics in the environment are also subjected to hydrolysis by β-lactamase enzymes, which can be secreted by the cell.[30] This study showed for the first time that it is possible to overcome drug resistance through the combined delivery of silver nanoparticles and ampicillin. Co-encapsulation resulted in synergistic activity sufficient to delay or inhibit the growth of bacteria, even when the gene for ampicillin resistance was present. The authors postulate that the effectiveness of this formulation is most likely due to a mechanism which exploits the reactive properties of nanoscale silver in order to disrupt the integrity of outer cell membrane. This is supported by the observation that silver nanoparticles can cause morphological changes and indentation of the bacteria cell wall.[31] Membranes with the observed morphology have been reported to exhibit a significant increase in permeability, resulting in abnormal transport across the membrane.[32] Silver ions have also been well documented to form reactive oxygen species (ROS), which can likewise cause damage to bacteria cell walls and subsequent cell death.[22] The mechanism of synergism is under further investigation by the authors.

This work has many important implications. A long-lasting, single-particle treatment capable of overcoming antibiotic resistance would be extremely beneficial in the clinic. This potential is compounded by the fact that the initial bacteria density found *in vivo* is rarely as high as the CFU studied here. It has been shown that silver nanoparticles are also effective at treating bacterial persister cells, and therefore AgPs may show promise for biofilm-forming infections.[33-34] One of the most commonly occurring bacterial infections, urinary tract infection, is frequently caused and perpetuated by biofilm-forming (and often antibiotic-resistant) strains of *E. coli*.[35] Additionally, the absence of a significant cytotoxic effect from AgPs towards human fibroblasts is a promising sign for toleration by mammalian cells. Reports of toxicity associated with nanoscale silver *in vivo* have been varied, and toxicity is generally considered to depend on nanoparticle size, concentration, and surface coating.[36-38] As designed, the AgPs particle is easily loaded with a variety of aqueous drugs, and combinations thereof, opening avenues for the creation of a library of therapeutic particles.

MATERIALS AND METHODS

Particle Synthesis

The antibiotic solution and silver nanoparticles were encapsulated inside the polymersomes by self-assembly. First, 1 mL of dodecanethiol-functionalized silver nanoparticles (5 ± 2 nm, 0.25% (w/v) in hexane; Sigma-Aldrich, St. Louis, MO) was resuspended in 1 mL of tetrahydrofuran (THF; Sigma-Aldrich, St. Louis, MO), and subsequently ultrasonicated (Bransonic 2510R-DTH, Emerson Industrial Automation, Danbury, CT) to prevent aggregation. 10 mg of the mPEG-PDLLA copolymer (Polyscitech, West Lafayette, IN) was added to the

mixture, which was again ultrasonicated until the copolymer was completely dissolved. This organic nanoparticle/polymer solution was then injected through a syringe atomizer (MAD300, LMA, San Diego, CA) into a 0.01 M solution of PBS (Sigma-Aldrich, St. Louis, MO) with or without ampicillin sodium salt (Sigma-Aldrich, St. Louis, MO) in a 15 mL glass round bottom tube with a 7x2 mm magnetic stir bar at 500 rpm. Finally, the entire polymersome solution was transferred to a 50 kDa dialysis tube (Spectra/Por Float-A-Lyzer G2, Spectrum Labs, Rancho Dominguez, CA) and was allowed to dialyze against pure PBS for 48 hours, with two buffer changes, to remove all traces of the organic solvent and unencapsulated drug.

Particle Characterization

The size distribution and zeta potential of AgPs were measured using DLS (90Plus Zeta, Brookhaven Instruments, Holtsville, NY) and the software provided by the manufacturer. Ampicillin loading efficiency was determined using a method previously described,[19] based on spectrophotometric optical density measurements at 320 nm (OD_{320}) (SpectraMax M3, Molecular Devices, Sunnyvale, CA) of a compound formed by the acidic degradation of ampicillin at 75 ºC in pH 5.2 buffer and a trace of copper (II) sulphate pentahydrate (Sigma-Aldrich, St. Louis, MO). Ampicillin concentration was measured directly after the synthesis process and after 48 hours of dialysis. Percentage loading efficiency was calculated as [final concentration] / [initial concentration] x 100%.

Transmission Electron Microscopy

AgPs and cell-particle interactions were visualized using transmission electron microscopy (TEM; JEM-1010, JEOL, Peabody, MA). Particles were dried on 300-mesh copper-

coated carbon grids (Electron Microscopy Sciences, Hatfield, PA) and negatively stained with a 1.5% uranyl acetate solution (Sigma-Aldrich, St. Louis, MO). Bacteria were treated with particles for 24 hours, fixed in 4% paraformaldehyde (Sigma-Aldrich, St. Louis, MO) for 30 minutes at 4 ºC, and absorbed on 300-mesh copper-coated carbon grids for imaging. Samples prepared for sectioning were fixed using 3% glutaraldehyde (Sigma-Aldrich, St. Louis, MO) and 2% paraformaldehyde, treated with 0.1% tannic acid, and postfixed with 1% osmium tetroxide (Electron Microscopy Sciences, Hatfield, PA) for 30 minutes. Following ethanol gradient dehydration, samples were infiltrated with polymer, cured, sectioned using an ultramicrotome (Reichert-Jung Ultracut E, Reichert Technologies, Buffalo, NY), and absorbed on 200-hex mesh copper-coated carbon grids (Electron Microscopy Sciences, Hatfield, PA) for imaging.

Bacteria Transformation

First, an overnight suspension of *E. coli* cells (strain K-12 HB101; Bio-Rad, Hercules, CA) was pelleted by centrifugation and re-suspended in 250 μL of cold 50 mM calcium chloride (Sigma-Aldrich, St. Louis, MO) and placed in an ice bath. After 15 minutes on ice, 10 μg of the plasmid DNA was added, and the cells were returned to the ice bath for an additional 15 minutes. The cells were then heat shocked by placing them in a 42 ºC water bath for exactly 45 seconds and then rapidly transferring them back to the ice bath for 2 minutes. This solution was then mixed with 750 μL of Lysogeny broth (LB, Sigma-Aldrich, St. Louis, MO). Finally, the complete transformed bacteria solution was streaked for inoculation on a LB-agar plate containing 100 μg/mL of ampicillin and allowed to incubate overnight at 37 ºC.

Bacterial Interactions

For each experimental trial, a single bacterial colony was selected and grown overnight in LB on a shaking incubator set at 200 rpm and 37 ºC. The overnight bacterial suspension was adjusted by OD_{600} measurements and dilution to possess a final bacterial density of 10^6 CFU/mL. 100 µL of the bacterial suspension was then combined with varying AgP treatment concentrations or controls in a 96 well plate. The final treatment volume in each well was brought up to 100 µL using 0.01 M PBS (*e.g.* 100 µL treatment + 0 µL PBS, 90 µL treatment + 10 µL PBS, 80 µL treatment + 20 µL PBS, *etc.*). Control treatments were given 100 µL of PBS to keep the media dilution consistent. The well plate was then allowed to incubate at 37 ºC inside a spectrophotometer under static conditions (SpectraMax Paradigm, Molecular Devices, Sunnyvale, CA). OD_{600} measurements were taken every 2 minutes for 24 hours to establish the speed of proliferation and shape of the bacterial growth curve. The differing base OD_{600} values for the various treatment types and concentrations were normalized by subtracting the read value from the value of a comparable blank solution.

Cytotoxicity

Cytotoxicity of the polymersome treatments towards human dermal fibroblast cells (Detroit 551 #CCL-110, American Type Culture Collection, Manassas, VA) was investigated via MTS assay (CellTiter 96® AQ_{ueous} One Solution Cell Proliferation Assay, Promega, Madison, WI). Experiments were carried out in DMEM (American Type Culture Collection, Manassas, VA) supplemented with 10% fetal bovine serum (American Type Culture Collection, Manassas, VA) and 1% penicillin-streptomycin (American Type Culture Collection, Manassas, VA). First, the cells were seeded into a 96 well plate at a density of $5x10^3$ cells/well ($\sim 1.5x10^4$ cells/cm^2) with 200 µL of media and allowed to adhere in an incubator at 37 ºC and 5% CO_2 for 24 hours.

13

The next day, the media was carefully aspirated from the wells and replaced with a mixture of 100 µL media and 100 µL of AgPs at various dilutions. The final treatment volume in each well was brought up to 100 µL using 0.01 M PBS (*e.g.* 100 µL treatment + 0 µL PBS, 90 µL treatment + 10 µL PBS, 80 µL treatment + 20 µL PBS, *etc.*). Control treatments were given 100 µL of PBS to keep the media dilution consistent. Following 24 and 48 hours of incubation at 37 ºC and 5% CO_2, the 200 µL treatment/media mixture was removed from each well and replaced with 200 µL of a 1:5 MTS reagent/media mixture. Finally, the plate was returned to the incubator for 4 hours, and the absorbance of each well was subsequently measured by spectrophotometer (SpectraMax M3, Molecular Devices, Sunnyvale, CA) at 490 nm.

Quantification of Synergy

The degree of drug synergism was determined using the Bliss Independence Model, in which $S = (f_{X0}/f_{00})(f_{0Y}/f_{00})-(f_{XY}/f_{00})$, where f_{00} is the wild-type bacteria growth rate in the absence of treatment; f_{X0} and f_{0Y} is the growth rate in the presence of individual drug at X or Y; f_{XY} is the growth rate in the presence of combined drugs X and Y; and S is the degree of synergy.[22,23] Given that the primary treatment response manifested as a dose-dependent delay in reaching exponential growth phase, here the growth rate was defined as the measured optical density divided by time. The drugs were considered to have a synergistic interaction when $S > 0$, and an antagonistic interaction when $S < 0$.

Statistical Analysis

All results were presented as the mean ± standard deviation unless otherwise noted, and all experiments were repeated at least in triplicate to demonstrate significance (N=3, n=3).

REFERENCES

1. Taubes G. The bacteria fight back. *Science*. 2008;321:356.

2. Rice, L. B. Emerging issues in the management of infections caused by multidrug-resistant gram-negative bacteria. *Cleve Clin. J. Med.* 74, S12–S20 (2007).

3. Antibiotic Resistance Threats in the United States, 2013. Centers for Disease Control and Prevention.

4. Pages JM, James CE, Winterhalter M. The porin and the permeating antibiotic: a selective diffusion barrier in Gram-negative bacteria. *Nature Reviews Microbiology*. 2008;6:893.

5. Norrby SR, Nord CE, Finch R. Lack of development of new antimicrobial drugs: a potential serious threat to public health. *The Lancet Infectious Diseases*. 2005;5(2):115-119.

6. Lee JS. Polymersomes for drug delivery: Design, formation and characterizations. *J. Control. Release.* 161 (2012) 473-483.

7. Hoiby N, Bjarnsholt T, Givskov M, Molin S, Ciofu O. Antibiotic resistance of bacterial biofilms. *Int. J. Antimicrob. Agents*. 2010;35:322-332.

8. Nacucchio MC, Bellora MJ, Sordelli DO, D'Aquino M. Enhanced liposome-mediated activity of piperacillin against staphylococci. *Antimicrob. Agents Chemother.* 1985;27:137-139.

9. Alhajlan M, Alhariri M, Omri A. Efficacy and safety of liposomal clarithromycin and its effect of *Pseudomonas aeruginosa* virulence factors. *Antimicrob. Agents Chemother.* 2013;57:2694-2704.

10. Geilich BM, Webster TJ. Reduced adhesion of *Staphylococcus aureus* to ZnO/PVC nanocomposites. *Int. J. Nanomed.* 2013;8:1177-1184.

11. Magner LN. In: Hippocrates and the Hippocratic Tradition. A History of Medicine. Duffy J, editor. Marcel Dekker, Inc; NYC: 1992. p. 393.

12. Shrivastava S, Bera T, Roy A, Singh G, Ramachandrarao P, Dash D. Characterization of enhanced antibacterial effects of novel silver nanoparticles. *Nano.* 2007;18:225103.

13. Shahverdi AR, Fakhimi A, Shahverdi HR, Minaian S. Synthesis and effect of silver nanoparticles on the antibacterial activity of different antibiotics against *Staphylococcus aureus* and *Escherichia coli*. *J. Nano.* 2007;3(2):168-171.

14. Li P, Li J, Wu C, Wu Q, Li J. Synergistic antibacterial effects of ß-lactam antibiotic combined with silver nanoparticles. *Nano*. 2005;16(9):1912.

15. Fayaz AM, Balaji K, Girilal M, Yadav R, Kalaichelvan PT, Venketesan R. Biogenic Synthesis of Silver Nanoparticles and their Synergistic Effect with Antibiotics: A Study Against Gram-Positive and Gram-Negative Bacteria. *Nanomedicine: Nanotechnology, Biology and Medicine.* 2010;6(1):103-109

16. Li Y, Chen X, Gu N. Computational Investigation of Interaction between Nanoparticles and Membranes: Hydrophobic/Hydrophilic Effect. *J. Phys. Chem. B.* 2008;112:16647-16653.

17. Scott, MD, Murad KL, Koumpouras F, Talbot M, Eaton JW. Chemical camouflage of antigenic determinants: Stealth erythrocytes. *Proc. Natl. Acad. Sci.* 1997;94:566-7571.

18. Santin M. Strategies in Regenerative Medicine: Integrating Biology with Materials Design. Springer. 2009:62.

19. Smith JWG, Grey GE, Patel VJ. Spectrophotometric Determination of Ampicillin. *Analyst*. 1967;92:247-252.

20. Froger A, Hall JE. Transformation of Plasmid DNA into *E. coli* Using the Heat Shock Method. *J Vis Exp.* 2007;6:253.

21. Matagne A, Lamotte-Brasseur J, Frere JM. Catalytic properties of class A beta-lactamases: efficiency and diversity. *Biochem. J.* 1998;330(2):581-598.

22. Morones-Ramirez JR, Winkler JA, Spina CS, Collins JJ. Silver Enhances Antibiotic Activity Against Gram-Negative Bacteria. *Sci Transl Med*. 2013;5(190).

23. Hegreness M, Shoresh N, Damian D, Hartl D, Kishony R. Accelerated evolution of resistance in multidrug environments. *Proc. Natl. Acad. Sci. U. S. A.* 2008;105:13977.

24. Feng QL, Wu J, Chen GQ, Cui FZ, Kim TN, Kim JO. A mechanistic study of the antibacterial effect of silver ions on *Escherichia coli* and *Staphylococcus aureus*. *J. Biomed. Mater. Res.* 2000;52(4):662-668.

25. Liau SY, Read DC, Pugh WJ, Furr JR, Russell AD. Interaction of silver nitrate with readily identifiable groups: relationship to the antibacterial action of silver ions. *Lett. Appl. Microbiol.* 1997;25(4):279-283.

26. Nikaido H, Vaara M. Molecular Basis of Bacterial Outer Membrane Permeability. *Microbiological Reviews*. 1985;49(1):1-32.

27. Silva MT, Sousa JC. Ultrastructure of the Cell Wall and Cytoplasmic Membrane of Gram-Negative Bacteria with Different Fixation Techniques. *Journal of Bacteriology*. 1973;113(2):953-962.

28. Raetz CR. Biochemistry of Endotoxins. *Annual Review of Biochemistry*. 1990;59(1):129-170.

29. Lim SP, Nikaido H. Kinetic Parameters of Efflux of Penicillins by the Multidrug Efflux Transporter AcrAB-Tolc of *Escherichia coli. Antimicrob. Agents Chemother.* 2010;54(5):1800-1806

30. Chervaux C, Sauvonnet N, Le Clainche A, Kenny B Hung AL, Broome-Smith JK, Holland IB. Secretion of active beta-lactamase to the medium mediated by the *Escherichia coli* haemolysin transport pathway. *Mol. Gen. Genet.* 1995;249(2):237-245.

31. Kim JS, Kuk E, Yu KN, Kim J, Park SJ, Lee HJ, Kim SH, Park YK, Park YH, Hwang C, *et al.* Antimicrobial Effects of Silver Nanoparticles. *Nanomedicine: Nanotechnology, Biology and Medicine*. 2007;3(1):95-101.

32. Sondi I, Salopek-Sondi B. Silver Nanoparticles as Antimicrobial Agent: A Case Study on *E. coli* as a model for Gram-negative bacteria. *Journal of Colloid and Interface Science*. 2004;275(1):177-182.

33. Kalishwaralal K, BarathManiKanth S, Pandian SRK, Deepak V, Gurunathan S. Silver Nanoparticles Impede the Biofilm Formation by *Pseudomonas aeruginosa* and *Staphylococcus epidermidis*. *Colloids and Surfaces B: Biointerfaces*. 2010;79(2):340-344

34. Roe D, Karandikar B, Bonn-Savage N, Gibbins B, Roullet J. Antimicrobial Surface Functionalization of Plastic Catheters by Silver Nanoparticles. *Journal of Antimicrobial Chemotherapy*. 2008;61(4):869-876.

35. Mah T. Biofilm-Specific Antibiotic Resistance. *Future Microbiology.* 2012;7(9):1061

36. AshaRani PV, Mun GLK, Hande MP, Valiyaveettil S. Cytotoxicity and Genotoxicity of Silver Nanoparticles in Human Cells. *ACS Nano.* 2009;3(2):279-290.

37. Ahamed M, AlSalhi MS, Siddiqui MKJ. Silver nanoparticle applications and human health. *Clinica Chimica Acta*. 2010;411(23-24):1841-1848.

38. Lima R, Seabra AB, Durán N. Silver nanoparticles: a brief review of cytotoxicity and genotoxicity of chemically and biogenically synthesized nanoparticles. *J. Appl. Toxicol.* 2012;32:867-879.

ACKNOWLEDGEMENTS

FIGURES, TABLES, AND EQUATIONS

<u>Figures</u>
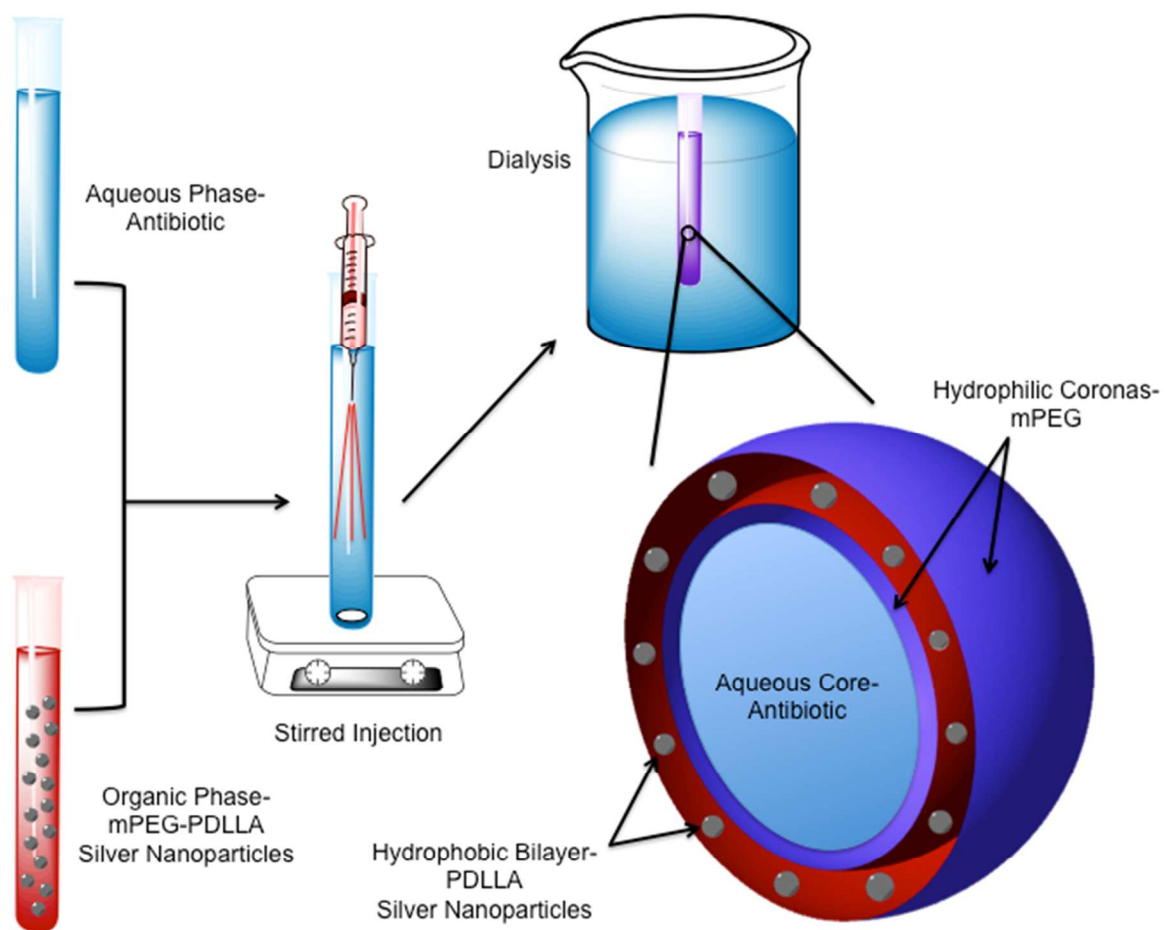
Figure 1. **Particle synthesis.** A solution of the mPEG-PDLLA copolymer and hydrophobically-functionalized silver nanoparticles in organic solvent (red) is injected through a syringe atomizer into a stirring aqueous solution of ampicillin sodium salt in PBS (blue). The organic solvent and any unencapsulated drug are subsequently removed by dialysis.
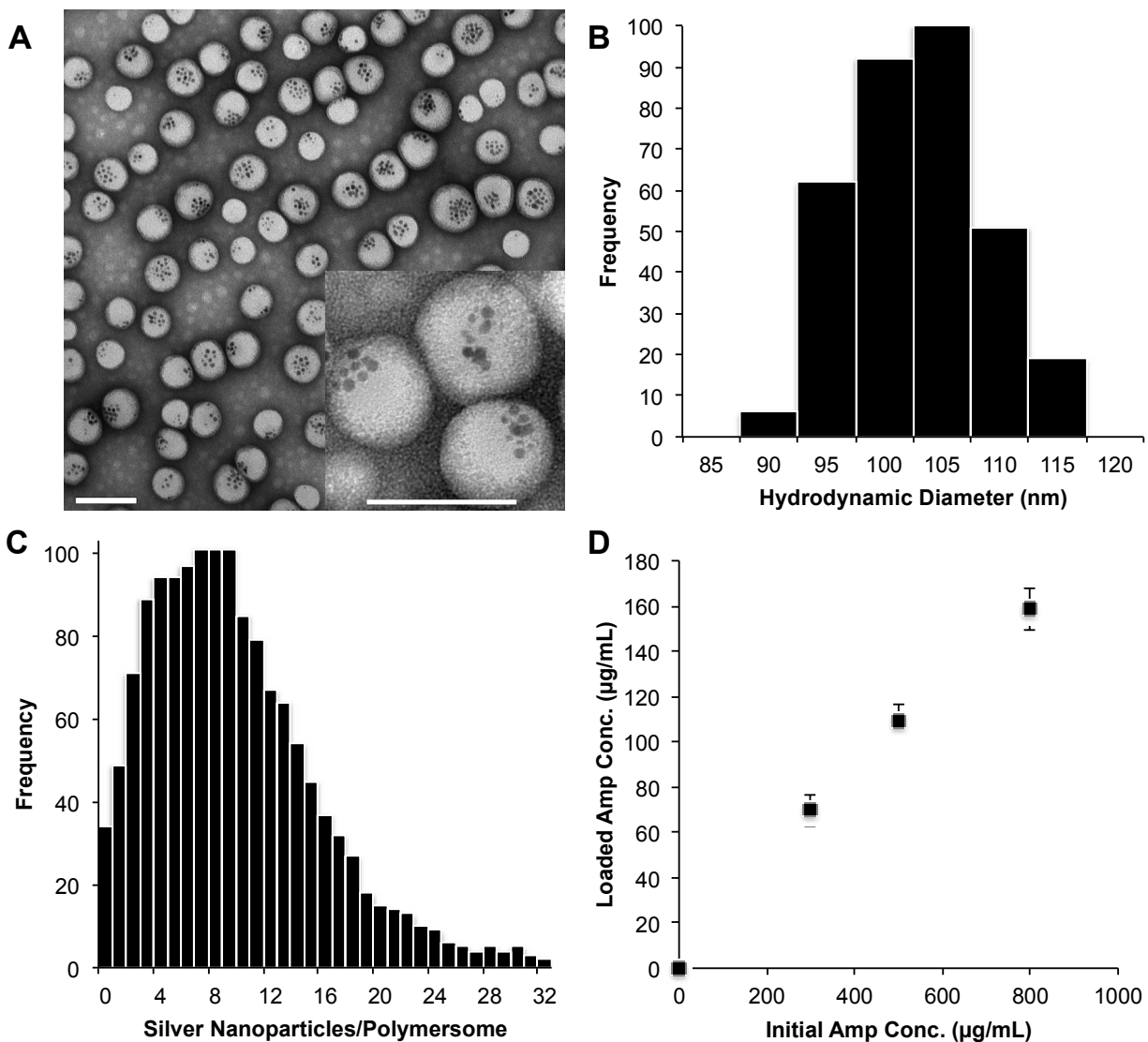
Figure 2. Physiochemical characterization. (a) Transmission electron micrographs reveal the presence of the 5 nm silver nanoparticles (dark dots) embedded within the larger polymersome particles. Scale bars = 100 nm. (b) The size distribution of the AgPs was measured using dynamic light scattering at 25 ºC. Results indicate an average particle size of 104.3 nm ± 15.6 nm. (c) Examination of TEM images show that an average of 9.29 ± 6.07 silver nanoparticles were loaded per polymersome. (d) The final concentration of ampicillin present in AgPs was determined to be 70 µg/mL ± 7.0 µg/mL (1 Ag:0.28 Amp) , 110 µg/mL ± 7.2 µg/mL (1 Ag:0.44

Amp), and 160 µg/mL ± 9.0 µg/mL (1 Ag:0.64 Amp), corresponding to a loading efficiency of

23%, 22%, and 20% respectively. Values represent the mean ± standard deviation.
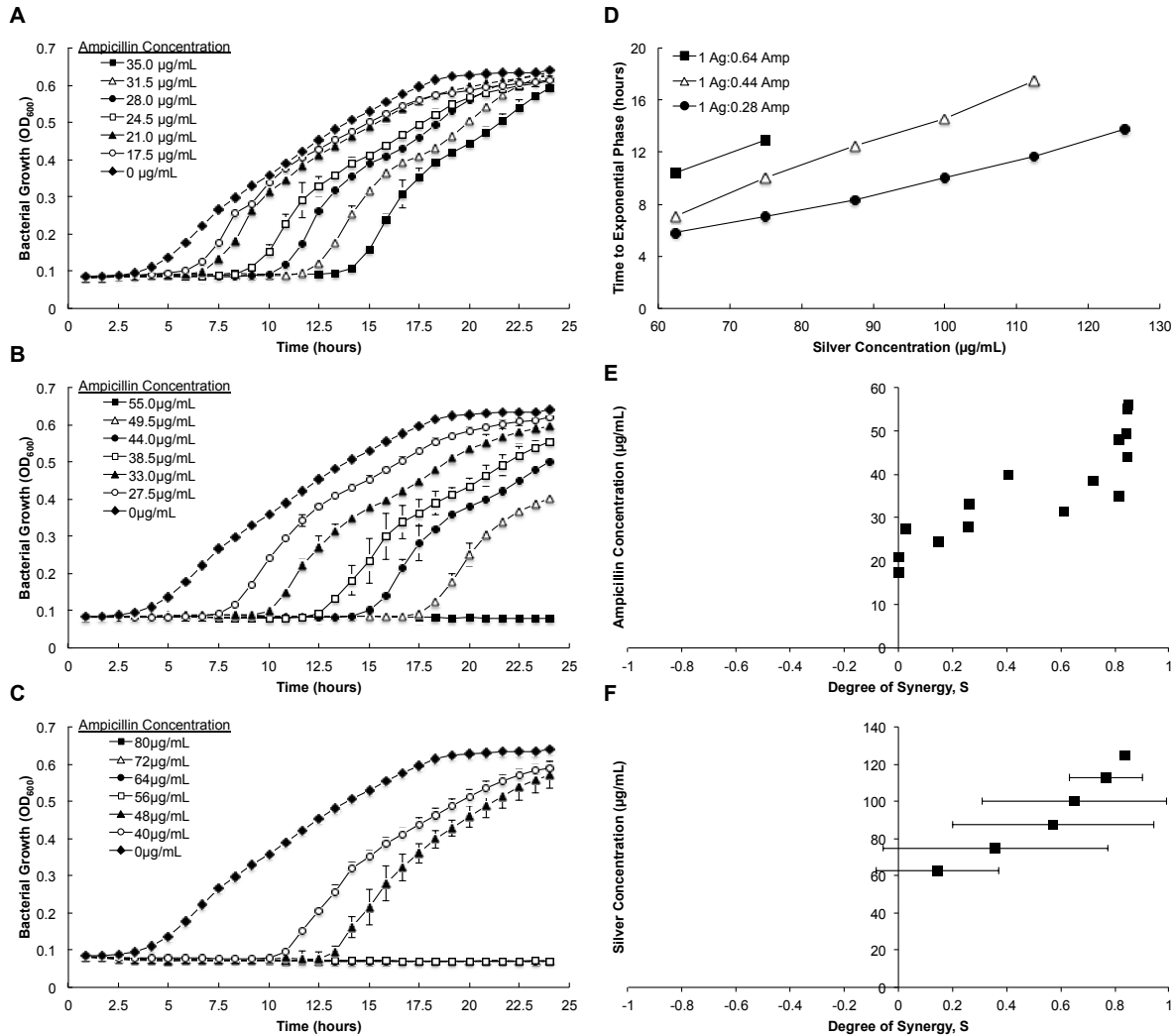

Figure 3. Bacterial growth inhibition. The proliferation of a 10^6 CFU/mL suspension of

antibiotic-resistant *E. coli* was measured over 24 hours in the presence of differing

concentrations of AgPs loaded with (a) 1 Ag:0.28 Amp, (b) 1 Ag:0.44 Amp, (c) and 1 Ag:0.64

Amp. Values represent the mean ± standard deviation (d) The time taken for the bacteria to reach

exponential phase was compared between treatment groups. The *in vitro* synergy between the

silver and ampicillin during log-linear growth phase was determined at 13.3 hours by the Bliss

Independence model. Synergism is observed for (e) increasing concentrations of ampicillin and

(f) silver nanoparticles.
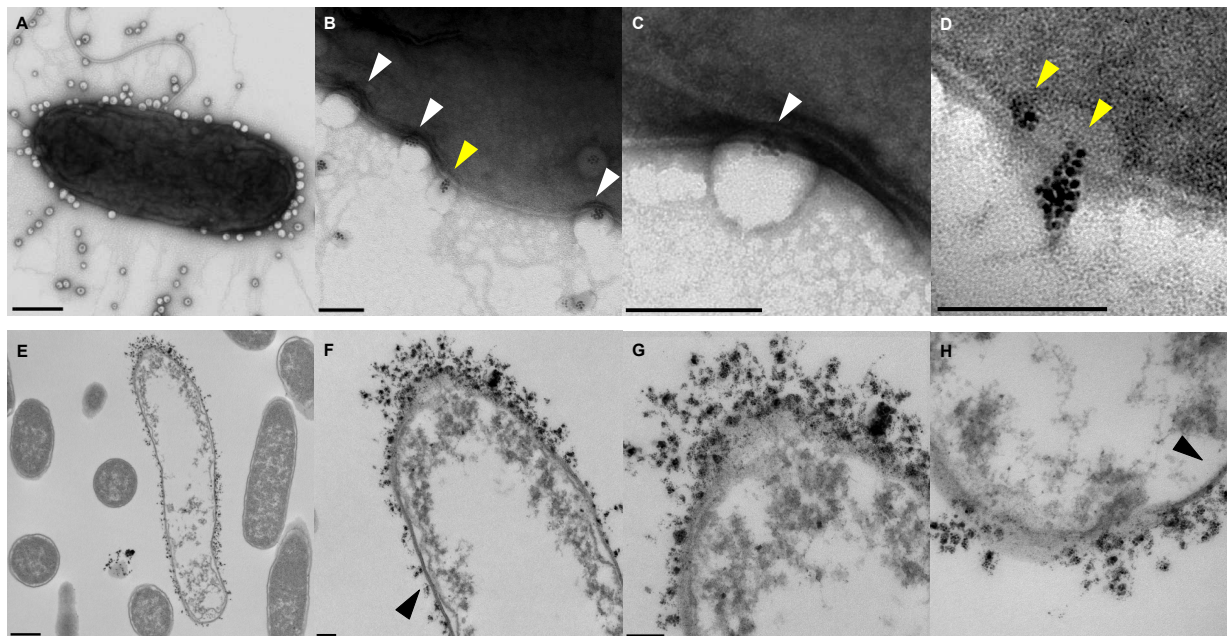
Figure 4. Bacteria-particle interactions. Transmission electron micrographs of whole bacteria

(a-d) and thin sections (e-h) after AgPs treatment. (a-d) Indentation of the bacterial cell

membrane was observed in regions of AgPs contact (white arrows). Silver nanoparticles inside

AgPs exhibit signs of polarization indicative of hydrophobic interactions (yellow arrows). (e-h)

Bacteria in contact with AgPs displayed significant protein aggregation and membrane

disruption. Regions of the outer membrane with little AgPs contact appear morphologically

normal (black arrows). Scale bars = 100 nm (a-d, f-h) and 500 nm (e).
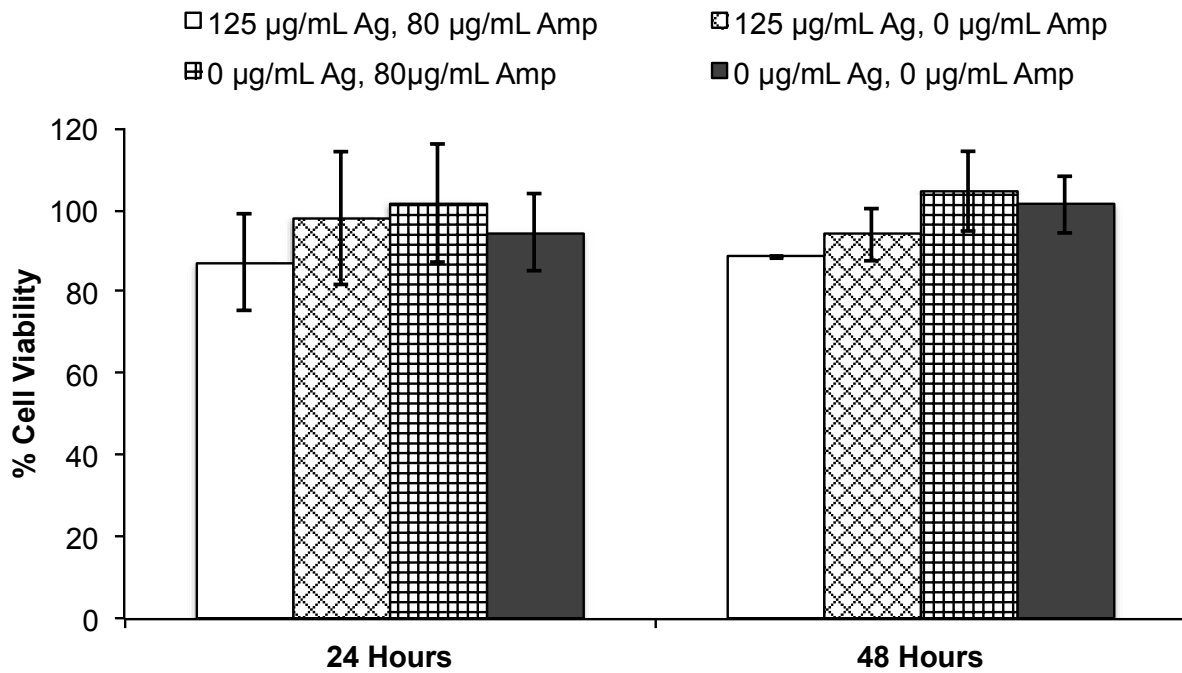
Figure 5. Particle cytotoxicity. The viability of CCL-110 human dermal fibroblast cells following 24 and 48 hours treatment with varying concentrations of AgPs as assessed via MTS assay. The treatment concentration displayed corresponds to the highest bacterial treatment concentration tested (1 Ag:0.64 Amp). No significant cytotoxicity was observed. Values represent the mean ± standard deviation.

Tables

Mass Ag	Per mL AgP Solution	Per Silver Nanoparticle	Per Average AgP
g	2.5×10^{-4}	6.9×10^{-19}	$6.4 \times 10^{-18} \pm 4.1 \times 10^{-18}$
mol	2.3×10^{-6}	6.4×10^{-21}	$5.9 \times 10^{-20} \pm 3.8 \times 10^{-20}$
atoms	1.4×10^{18}	3.8×10^{3}	$3.6 \times 10^{4} \pm 2.3 \times 10^{4}$

Table 1. Quantification of the amount of silver delivered per nanoparticle and per AgP.

Equations

$$(4/3)\pi(r)^3 = (4/3)\pi(2.5nm)^3 = 65.45nm^3 = 6.545\times10^{-20}cm^3 \text{ volume per nanoparticle (1)}$$

$$10.49g/cm^3 \times 6.545\times10^{-20}cm^3 = 6.866\times10^{-19}g \text{ silver per nanoparticle (2)}$$

$$6.866\times10^{-19}g \ / \ 107.8682g/mol = 6.365\times10^{-21}mol \text{ silver per nanoparticle (3)}$$

$$6.365\times10^{-21}mol \times 6.022\times10^{23} \text{ atoms/mol} = 3.833\times10^3 \text{ silver atoms per nanoparticle (4)}$$